Environmental Engineering and Management Journal

December 2018, Vol.17, No. 12, 2807-2814
http://www.eemj.icpm.tuiasi.ro/; http://www.eemj.eu

"Gheorghe Asachi" Technical University of Iasi, Romania

VOLTAMMETRIC STUDIES OF $YBaCo_2O_5$ IN ALKALINE AQUEOUS SOLUTION

Mircea Dan, Andrea Kellenberger, Nicolae Vaszilcsin, Narcis Duteanu*

University "Politehnica" of Timisoara, Faculty of Industrial Chemistry and Environmental Engineering, P-ta Victoriei 2, 300006 Timisoara, Romania

Abstract

Electrochemical behaviour of $YBaCo_2O_5$ perovskite in alkaline solution was studied during oxygen insertion/release process. In correlation with electrochemical studies was analyzed the compound morphology and structure. Compound electrochemical oxidation consists in intercalation of oxygen atoms in crystalline structure, which is equivalent with a structure compaction. These results were correlated with the Brunauer-Emmett-Teller (BET) surface area of sample and also with SEM pictures.
Compaction of Y-112 crystalline structure during electrochemical oxidation leads at some partial irreversible character of studied process. Presence of a chemical step during electrochemical oxidation of studied perovskite was emphasized from electrochemical impedance data. This step was associated with O^{2-} ions formation. Based on the obtained results a mechanism of electrochemical oxidation/reduction of $YBaCo_2O_5$ perovskite in alkaline solution was proposed.

Key words: BET technique, cyclic voltammetry, electrochemical behaviour of $YBaCo_2O_5$, mixed oxides, $YBaCo_2O_5$

Received: October, 2014; Revised final: March, 2015; Accepted: March, 2015; Published in final edited form: November 2018

1. Introduction

Actual challenge for solid oxide fuel cells (SOFC) technology is represented by the development of new electrode materials with high conductivity. Due to the major voltage losses on the cathodic side of the SOFC, experimental studies are carried out in accordance with that (Bebelis et al., 2007; Doubova et al., 2009; Liu, 2009; Sajana et al., 2017; Therese et al., 2005). In practice, the catalytic activity for oxygen reduction reaction is heavily affected by the temperature reduction. Considering this it is vital to develop a new class of high performance cathodes with important catalytic activity and also with low overpotential (Bebelis et al., 2007; Doubova et al., 2009; Liu, 2009; Lv et al., 2007; Wackerl et al., 2009). A suitable candidate is represented by a new class of perovskite – like compounds, $MBaCo_2O_{5+\delta}$ (M =Y, Gd, Pr). This new class of compounds has an 112 phases (Liu, 2009) and from structural point of view they present a layered structure (Bobrovskii et al., 2009; Liu, 2009). Bobrovskii et al. (2009) demonstrate that the compound structure is derived from orthorhombic structure of 112 perovskites, where on crystalline lattice, *c* axis is stacked sandwiches of CoO_2–BaO–CoO_2–MO_x. In these structure the CoO_2 layers are separated by the MO_x layer (Bobrovskii et al., 2009) which induces some remarkable properties (Liu, 2009). Actually, the MOx layer is acting like a carrier for charge donors (Bobrovskii et al., 2009; Tarancon et al., 2010), and is expected that the oxygen transport via perovskite layer is easy (Liu, 2009; Tarancon et al., 2010). Boborvskii et al. (2009) demonstrate that the system charge can be easy controlled only by changing oxygen concentration into the intermediate oxide layers.

Oxygen content in $YBaCo_2O_5$ can be easily modified by temperature, surrounding oxygen partial pressure, and also by oxygen intake/release mechanism into the perovskite network which

* Author to whom all correspondence should be addressed: e-mail: narcis.duteanu@chim.upt.ro

translates in variation of physical and chemical properties of the compound. This causes variations among the most important oxygen transport properties like oxygen nonstoichiometry, oxygen ion permeability and diffusion, which must be regarded as a highly important issue when studying perovskite-like oxides (Haoshan et al., 2007).

However, in the majority of practical studies until now, the oxygen transport properties of $YBaCo_2O_5$ were investigated by direct oxygen permeation measurement through a membrane, electrical conductivity measurement, coulometric relaxation method, isotopic exchange analysis, revealing the perovkite structure (Haoshan et al., 2007; Liu, 2009; Pelosato et al., 2014; Wackerl et al., 2009; Zhang et al., 2007).

The aim of this paper is to study and elucidate the electrochemical behaviour of $YBaCo_2O_5$ perovskite in aqueous alkaline solution. Given the possibility of electrochemical intercalation of oxygen atoms in cobaltites, the alkaline medium was chosen (Dan et al., 2011; Grenier et al., 1999; Grenier et al., 1992). Regarding the electrochemical studies presented in this paper, it is relevant to mention that in each unit cell there are two different Co cations, Co(II) and Co(III), with an atomic ratio of 1:1 as well as that the electrochemical behavior of Y-112 is determined by the mixed ionic and electronic conductivity (Aurelio et al., 2007; Haoshan et al., 2007; Kim and Manthiram, 2008; Zhang et al., 2008; Zhang et al., 2007). Due to the presence of Co^{2+} which oxidizes to Co^{3+} during the electrochemical process of adsorption, the structure is allowing the intake of ½ O, as oxygen adsorption takes place by permitting the oxygen diffusion into the oxides network and bonding an oxygen atom to two cobalt atoms from neighboring unit cells.

Until now the oxidation capacity of Y-112 compound and also the reversibility of the oxidation process has been studied using only thermogravimetric measurements carried out under oxygen flow. Thus, oxidation capacities of the compound up to $YBaCo_2O_{5+\delta}$, where $\delta = 1.0$ were obtained (Aurelio et al., 2007; Haoshan et al., 2007; Kim and Manthiram, 2008; Zhang et al., 2008; Zhang et al., 2007)

2. Material and methods

The mixed oxide $YBaCo_2O_5$ was obtained using solid state reaction by mixing the precursors Y_2O_3 (Aldrich 99.99%), $BaCO_3$ (Aldrich 99.999%) and $CoO_{4/3}$ (Normapur 99.9%) according to the stoichiometric cations ratio. After decarbonisation at 900°C the powder was pressed into pellets with geometrical active surface area of 1 cm^2 and later fired in air for 48 h at 1100°C and then removed rapidly from furnace and set to ambient temperature (Haoshan et al., 2007; Kim and Manthiram, 2008; Liu, 2009; Zhang et al., 2007). Surface morphology of $YBaCo_2O_5$ samples has been characterized by scanning electron microscopy (SEM) using a FEI INSPECT S PANalytical microscope coupled with energy dispersive X-ray detector. The structure of obtained $YBaCo_2O_5$ compound (Fig.1) was checked by X-Ray powder diffraction (Philips X-pert Pro).

All electrochemical studies were carried out using an Autolab PGSTAT 302N. The electrochemical cell was equipped with two graphite counter electrodes positioned symmetrically against the working electrode ($YBaCo_2O_5$ pellets) and a Ag/AgCl reference electrode. All potentials in this work are given versus the reference electrode. Cyclic voltammograms (CV) have been recorded at several scan rates in 1 mol L^{-1} KOH electrolyte solution. Electrochemical impedance spectoscopy (EIS) measurements were carried out using an Autolab 302N in the frequency range from 0.001 Hz to 100 kHz and an AC voltage amplitude of 10 mV. Each spectrum consisted of 60 points collected with a logarithmic distribution of 10 points per decade. Electrochemical impedance data were fitted to the electrical equivalent circuit by a complex nonlinear least squares (CNLS) Levenberg-Marquardt procedure using ZView Scribner Associated Inc. software.

The surface area was determined according to the Brunauer-Emmet-Teller (BET) method using an ASAP 2020 M (Micromeritics Instrument Corporation USA). Thermogravimetric (TG) studies were carried out using an NETZSCH TG 209F1 Libra microbalance, when 50 mg of mixed oxide was heated in two different gases (pure nitrogen and also pure oxygen) up to 1000 °C with a heating rate of 5°C min^{-1}.

3. Results and discussion

3.1. Physical characterization

The structure of mixed oxide is presented in Fig. 1 and it was investigated by X-ray powder diffraction. X-ray diffraction spectra for obtained $YBaCo_2O_5$ mixed oxide were recorded for the 2θ range between 0° and 100° and are presented in Fig. 2. Peaks from recorded diffraction pattern were identified and this it can be concluded that the obtained compound is $YBaCo_2O_5$ mixed oxide. Simultaneously the elemental composition of mixed oxide was confirmed by energy dispersive X-Ray analysis (EDX) as it can be observed in Fig. 3.

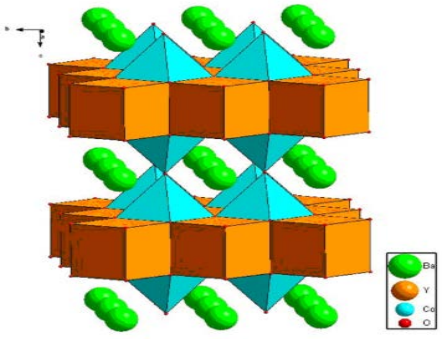

Fig. 1. Crystal structure of $YBaCo_2O_5$ perovskite

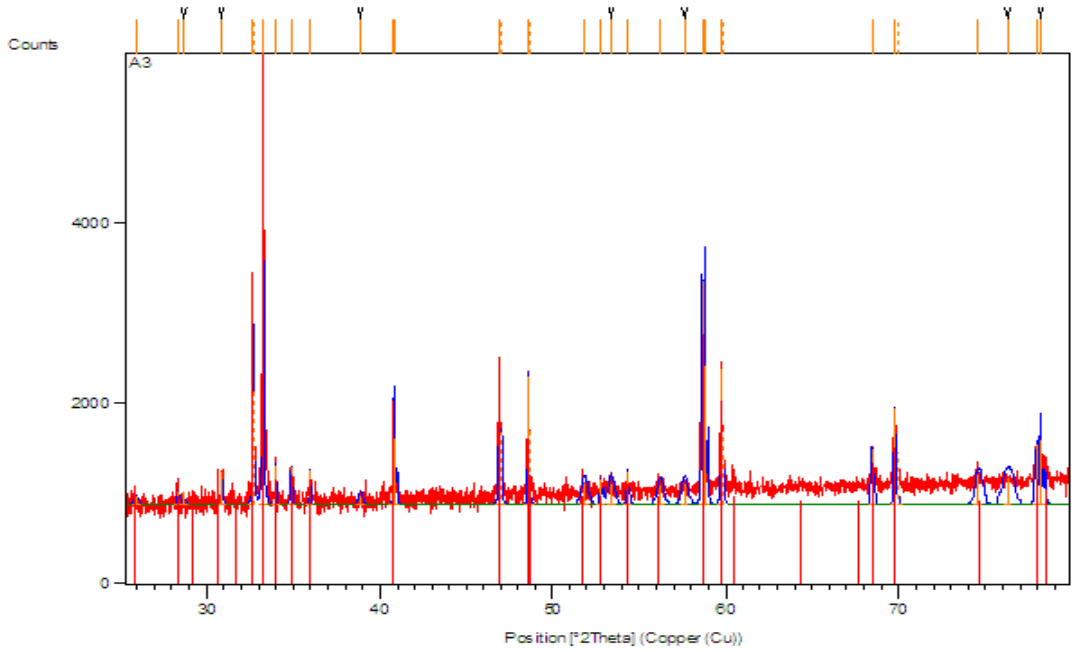

Fig. 2. XRD spectra recorded for $YBaCo_2O_5$ perovskite

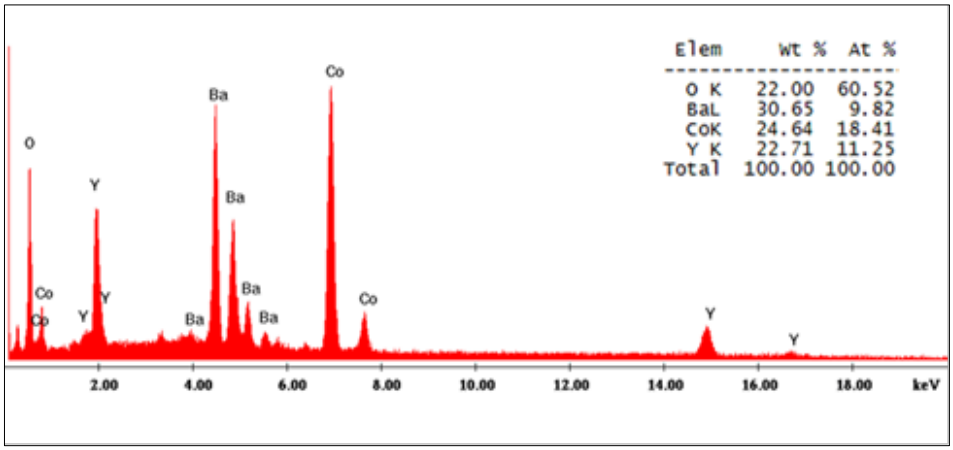

Fig 3. EDX spectra recorded for $YBaCo_2O_5$ perovskite

The compound porosity was determined by the BET technique and the results are presented in Table 1. The results indicate a large specific surface area, with pores and channels that can favour adsorption and desorption of oxygen during electrochemical polarization.

Table 1. BET surface area, pore diameter, and pore volume of the $YBaCo_2O_5$ sample

BET Surface Area [m^2 g^{-1}]	0.22
BJH Desorption average pore diameter (4V/A) *[nm]*	10.25
BJH Desorption cumulative volume of pores between 1.7000 nm and 300.0000 nm diameter [cm^3 g^{-1}]	0.000696

Compared with a dense bulk sample, is expected that this porous structure shows fast oxygen adsorption and desorption rates.

Results obtained from TG-measurement are presented in Fig. 4.a as function of mass change versus temperature. From the TG plot recorded under nitrogen flux, the weight change observed is not significant, and also is reversible. This signifies that the studied compound is stable between 20°C and 1000°C. As was expected, the behaviour of studied perovskyte is different when TG studies were performed in pure oxygen flow (results depicted in Fig. 4.b). An increase of mass with 1% can be observed around 400°C. These can be associated with oxygen diffusion inside of mixed oxide. Also, it observed that the weight variation is reversible.

An important factor influencing the oxidation process kinetics is the surface morphology which has been analyzed using scanning electron microscopy. SEM images obtained for $YBaCo_2O_5$ pellet electrode involved in this work are presented in Fig. 5. Analyzing the SEM image a porous structure due to acicular crystallites agglomeration can be observed.

Large pores amount leads to a higher specific surface with channels that favours oxygen adsorption / desorption process.

3.2. Electrochemical characterisation

Preliminary attempts have shown that it is possible to separate the peaks associated with the electrochemical processes occurring at the interface $YBaCo_2O_5$ – KOH 1 mol L^{-1} only if the potential scan rate is around 1 mV s^{-1}. The cyclic voltammograms recorded for $YBaCo_2O_5$ electrode are depicted in Fig. 6. Analyzing the voltammograms shown in Fig 6, it can be observed the appearance on the forward scan of an anodic peak (2) assigned to Co (II) oxidation ($Co^{II} \rightarrow Co^{III} + e^-$). At higher potentials the current increase (3) was associated with oxygen evolution reaction.

On the backward scan, a limiting anodic current with low intensity was observed (small peak 4), which was correlated with reduction of remanent oxygen on the electrode surface and also from the space between $YBaCo_2O_5$ crystallites.

When the potential becomes more negative, a cathodic peak (5) associated with Co (III) reduction process ($Co^{III} + e^- \rightarrow Co^{II}$) was recorded. The current increase (6) observed at more negative potential is associated with the hydrogen evolution reaction on perovskite electrode surface. Continuing the scan in the anodic direction from hydrogen evolution reaction zone until the open circuit potential (OCP), a new anodic peak (1) associated with oxidation of adsorbed hydrogen was observed at approximately -0.75 V versus Ag/AgCl.

Increasing the potential scan rate from 1mV s^{-1} to 10 mV s^{-1}, some changes in the anodic part of the cyclic voltammograms were observed. Analyzing the CV presented in Fig. 7, it can be noticed that the anodic peak (2) presented in Fig.6 was replaced with a net plateau which was associated with oxidation of Co (II) ions. The plateau current density is almost double compared with the height of peak (2) from Fig. 6.

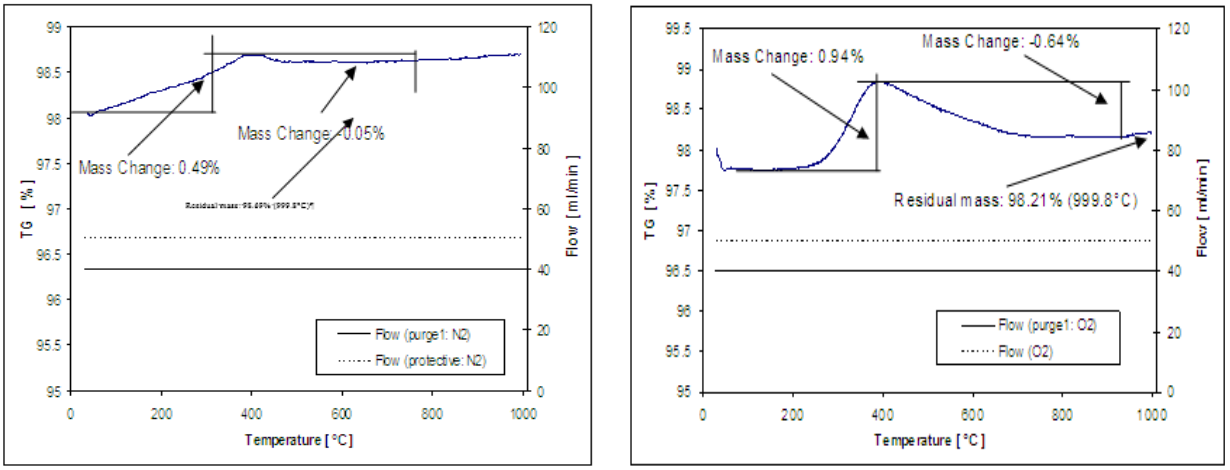

(a) (b)

Fig. 4. Thermogravimetric curves recorded in: (a) pure nitrogen, (b) pure oxygen

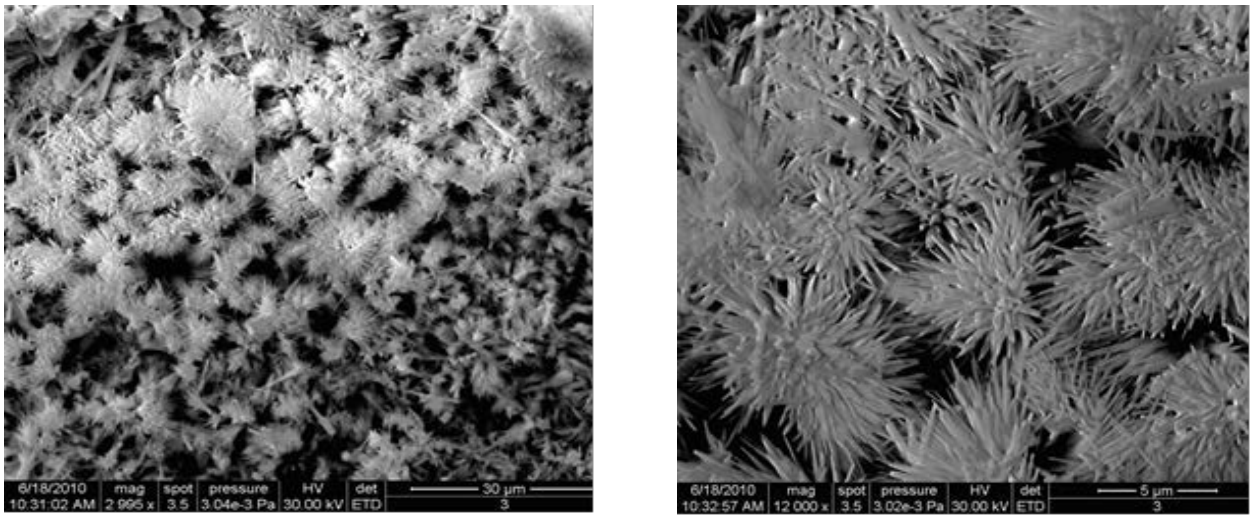

(a) (b)

Fig. 5. SEM images of $YBaCo_2O_5$ electrode's surface before electrochemical oxidation/reduction at 3000x (a) and 12000x (b) magnification

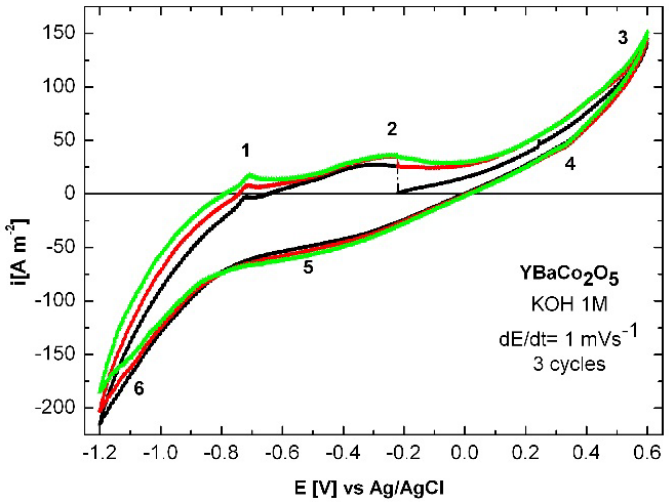

Fig. 6. Cyclic voltammograms on $YBaCo_2O_5$ working electrode in 1 mol L^{-1} KOH solution at 1 mV s^{-1} scan rate (cycle 1 – black color, cycle 2 – red color, cycle 3 – green color)

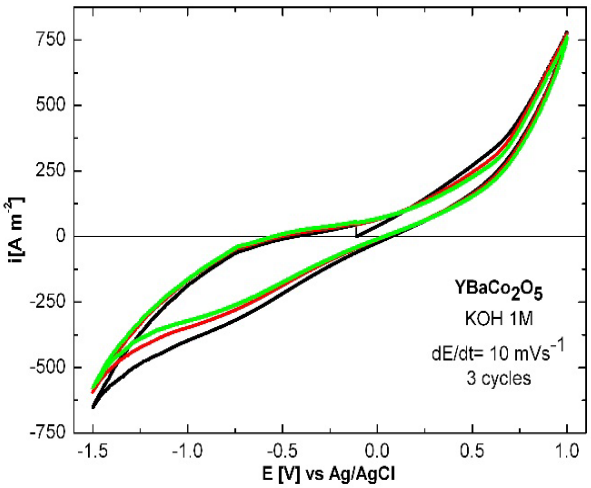

Fig. 7. Cyclic voltammograms on $YBaCo_2O_5$ working electrode in 1 mol L^{-1} KOH solution at 10 mV s^{-1} scan rate

When the CVs were recorded at much higher scan rate, for example at 50 mV s^{-1} (Fig. 8), the anodic part of the CV changes drastically, in this case the oxidation peak (2) and also the limiting current (peak 4) were not observed. This can be explained if we consider that the oxidation of $YBaCo_2O_5$ electrode occurs only at the electrode/electrolyte interface.

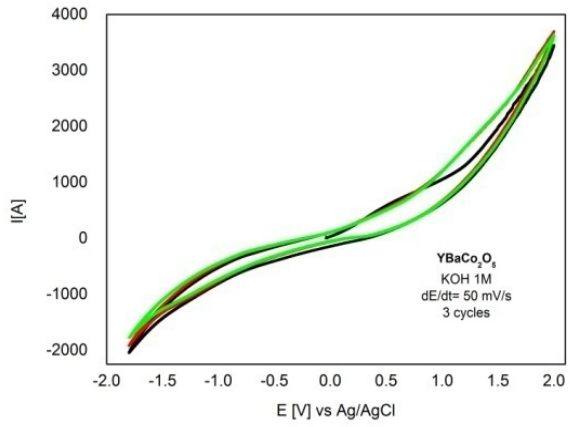

Fig. 8. Cyclic voltammograms on $YBaCo_2O_5$ working electrode in 1 mol L^{-1} KOH solution at 50 mV s^{-1} scan rate

Based on that we can conclude that the electrochemical oxidation of Co(II) ions to Co(III) ions actually consists in the insertion of oxygen ions into the $YBaCo_2O_5$ crystalline network. In consequence, during the electrochemical oxidation process, the crystalline network becomes more compact, and dense and in this way further oxygen diffusion into the network is limited. Later, the electrochemical behavior of the $YBaCo_2O_5$ electrode was studied using chronoamperometric techniques. In this case the working potential was set at -0.25 V (into the compound oxidation region), 0.00 V, 0.25 V (on the limiting current plateau) and also 0.50 V (at the potential corresponding to oxygen evolution reaction) versus Ag/AgCl reference electrode; these values were chosen in accordance with data obtained from $YBaCo_2O_5$ recorded CVs. The chronoamperometry data are depicted in Fig. 9. From data depicted in Fig. 9 was determinate the current variation as time function, representing a measure of compound oxidation in time. The values are presented in Table 2.

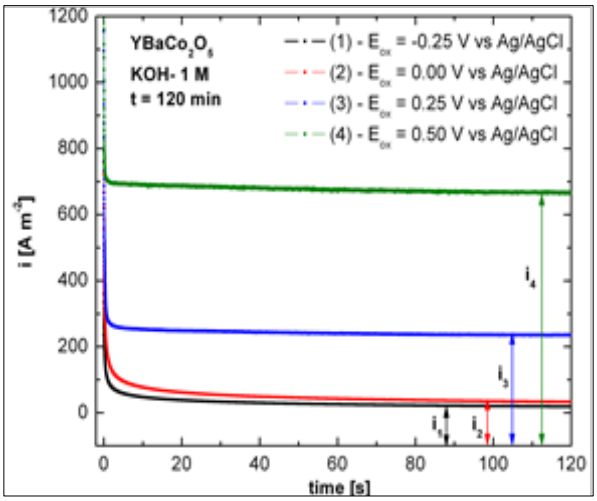

Fig. 9. Chronoamperometric data recorded on $YBaCo_2O_5$ electrode

Based on the data depicted in Fig.9 and also from Table 2 it can be stated that when the electrode potential was kept at -0.25 V and also at 0.00 V versus Ag/AgCl, on the working electrode surface can be observed only the perovskite oxidation. When the oxidation time is increasing, the current density becomes 0, due to the bulk or superficial oxidation of the $YBaCo_2O_5$ electrode, when the electrode surface was coated with a layer of $YBaCo_2O_{5+\delta}$ oxide (δ = max 0.5). Simultaneously with chronoamperometric data were recorded also the exact values of current used into the oxidation process.

Table 2. Final value of current measured from chronoamperometric data

E [V] vs Ag/AgCl	*i_{final} [A m^{-2}]*			
	t = 15 min	t = 30 min	t = 60 min	t = 120 min
- 0.25	41.92	33.27	35.56	18.53
0.00	67.67	53.94	42.49	32.81
0.25	250.34	247.00	239.97	234.56
0.50	688.76	682.34	674.38	665.84

Because, at -0.25 V and also at 0.00 V, the electrode oxidation consists only in Co(II) ions oxidation, it possible to calculate from electrolysis law the maximum oxygen content into the perovskite structure (Fig. 10).

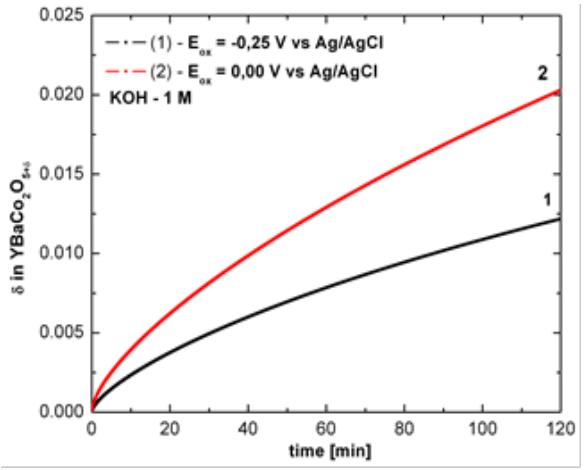

Fig. 10. Time variation of oxygen content

From the data presented in Fig. 10 can be observed that the increase of oxidation time is leading at some increase into the maximum oxygen content. For example, after 120 minutes (at 0.00V) the amount of oxygen is at 0.02 atoms / elemental cell, relatively to the maximum oxygen content of 0.011 atoms / elemental cell obtained after 45 minutes.

Based on the data presented above, an electrochemical mechanism for global oxidation process of $YBaCo_2O_5$ mixed oxide has been proposed. In accordance with this mechanism an oxygen activity gradient between superficial layer and bulk of mixed oxide occurs at anodic polarization of electrode. This leads to oxygen diffusion into the $YBaCo_2O_5$ crystal simultaneously with oxidation of Co(II) ions on the superficial layer. Oxidation of Co(II) ions onto the electrode surface and oxygen diffusion from electrode surface is equivalent with apparition of a superficial charge, compensated by the diffusion of hydroxyl ions from bulk of solution to the electrode surface. Presence of adjacent hydroxyl ions onto the electrode surface leads to formation of oxygen ions by water elimination.

This new oxygen ion will diffuse into the electrode bulk. EIS data demonstrate that the rate of oxygen diffusion into the perovskite structure is much lower than the rate of charge transfer reaction and the diffusion of hydroxyl ions to the interface (Dan et al., 2011).

At lower current densities, electrochemical mechanism for perovskite global oxidation takes place in two different stages. In first one, superficial Co (II) ions are oxidized at Co (III) ions in accordance with following reaction (Eq. 1):

$$Co_{(s)}^{2+} \rightarrow Co_{(s)}^{3+} + e^- \quad (1)$$

As an effect, an excess of positive superficial charges appears at interface. Interfacial charge is compensated by near hydroxyl ions which interact with interfacial Co^{3+} ions (Eq. 2):

$$HO_{(aq)}^- + Co_{(s)}^{3+} \rightarrow HO_{(ads)}^- \ldots Co_{(s)}^{3+} \quad (2)$$

At lower current densities, adsorbed hydroxyl concentration at interface is really small, so that the collision between two different adsorbed hydroxyl ions is not probable, even if the adsorbed HO^- ions are migrating over anode surface. More feasible are the collisions between adsorbed HO^- ions and the HO^- ions which are diffusing from bulk of solution to the electrode surface (Eq. 3):

$$HO_{(aq)}^- + HO_{(ads)}^- \ldots Co_{(s)}^{3+} \rightarrow O_{(ads)}^{2-} \ldots Co_{(s)}^{3+} + H_2O \quad (3)$$

When the current density is increasing, concentration of adsorbed HO^- ions is rising proportionally with current density, so the O^{2-} ion formation can also occur by collision between two different adsorbed HO^- ions (Eq. 4):

$$HO_{(ads)}^- \ldots Co_{(s)}^{3+} + HO_{(ads)}^- \ldots Co_{(s)}^{3+} \rightarrow Co_{(s)}^{3+} \ldots O_{(ads)}^{2-} \ldots Co_{(s)}^{3+} + H_2O \quad (4)$$

In accordance with proposed mechanism, oxidation of Co ions onto the electrode surface at anodic polarization near OCP is controlled by charge transfer reaction. At more positive potential, Co oxidation and oxygen ions bulk diffusion is controlled by the electrolyte diffusion.

Fig. 11 shows the EIS spectra for $YBaCo_2O_5$ electrode recorded during oxidation / reduction process. The main features of the complex plane impedance plots are the presence of a slightly curved line in the high frequency region, followed by diagonal line with a slope of 45° and a large semicircle in the low frequency region, which dominates the entire EIS spectra. The Bode plots obtained during oxidation at 0.125 V and reduction at -0.25 V have a slope of 0.5 and a phase angle value of 45° in the frequency range from 10 to 0.1 Hz which points to a diffusion controlled process. The impedance data have been modeled using a two-time constant equivalent electric circuit (EEC) given in Fig. 12. The EEC consists of a serial connection of the ohmic resistance (R_{Ohm}), a Gerischer element (Ge) and a parallel connection of a Warburg element (W) and a resistance (R) in series with a capacitor (C).

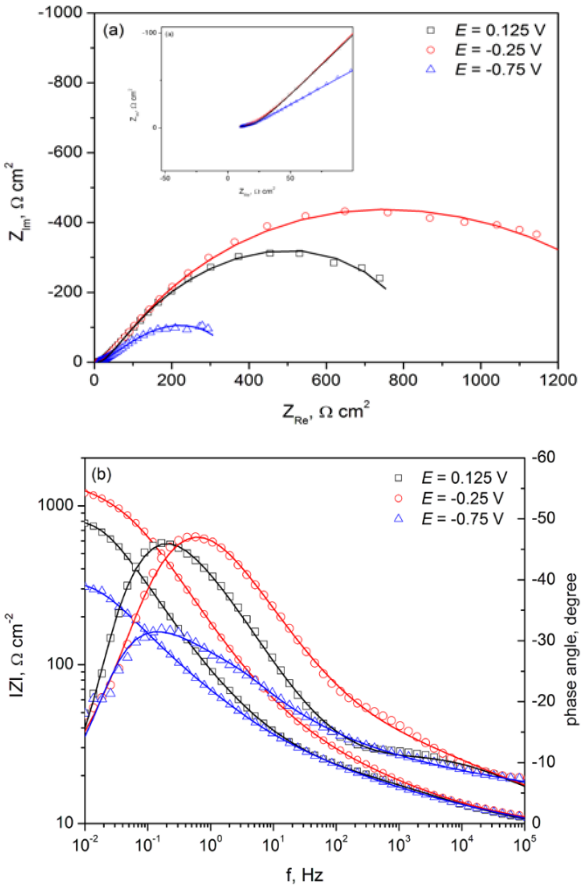

Fig. 11. Experimental Nyquist (a) and Bode (b) plots for YBaCo2O5 mixed oxide during oxidation / reduction. *Open symbols* are experimental points and *continuous lines* are simulated curves by the CNLS fitting according to the equivalent circuit

The ohmic resistance includes the uncompensated electrolyte resistance and a contribution from the resistance of $YBaCo_2O_5$ electrode. The inserting of a Gerischer element has been associated with systems involving a diffusion process coupled to a chemical reaction (Levi et al., 2004). In its most simple form, the impedance of a Gerischer element is given by (Eq. 5):

$$Z_{GE} = Z_0 / (k + j\omega)^{1/2} \quad (5)$$

where Z_o is the magnitude of the impedance at $\omega = 1$ rad s^{-1} and k is a rate constant of the chemical reaction.

The impedance of the Warburg element in case of a finite length thickness of the diffusion layer δ is given by (Eq. 6):

$$Z_w = (R_w(j\ \omega\tau_D)^{-\phi})\ \coth\ (j\ \omega\tau_D)^{\phi} \quad (6)$$

where R_w is the diffusion resistance, τ_D is the diffusion time constant given by $\tau_D = \delta^2/D$, with δ = diffusion layer thickness and D = diffusion coefficient and ϕ is an exponent between 0 and 1. This version of the Warburg element terminates in a finite resistance. At low frequencies, the real part of the Warburg impedance approaches R_W, and the imaginary part goes to zero. The EEC parameters obtained by fitting the experimental impedance data are listed in Table 3 together with their relative errors.

The Gerischer type impedance has been reported for a number of mixed conductors that can be used as anode or cathode materials in solid oxide fuel cells (González-Cuenca et al., 2001; Green et al., 2008; Kim et al., 2007; Nielsen et al., 2011) and it is generally ascribed to bulk diffusion and surface reaction kinetics. The closed values of the rate constant k and diffusion time constant τ_D obtained for the oxidation reaction indicate that both chemical and diffusion step control the overall process. During reduction, the diffusion of oxygen ions inside the solid host electrode is the rate determining step. Also, based on the diffusion time constant values it can be estimated that oxygen insertion during oxidation takes place faster than oxygen release during reduction.

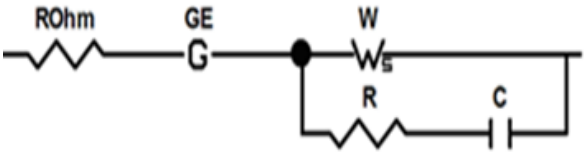

Fig. 12. Equivalent electric circuit for modeling oxygen insertion / release into the $YBaCo_2O_5$ electrode

4. Conclusions

The results obtained by cyclic voltammetry in alkaline aqueous solution showed that the $YBaCo_2O_5$ mixed oxide is sensitive to anodic or cathodic polarization. Based on the experimental data we can conclude that the electrochemical oxidation of Co(II) ions consists in oxygen insertion in the mixed oxide structure. As a result, during oxidation the Y-112 crystalline network becomes denser, so that oxygen diffusion rate is lowered.

Table 3. Fitted values of EEC during oxidation / reduction of $YBaCo_2O_5$

Parameter	E = 0.125 V	E = -0.25 V	E = -0.75 V
R_{Ohm} [Ω]	9.1 (1.6 %)	8.9 (2.0 %)	8.1 (1.6 %)
Z_0 [Ω cm² $s^{1/2}$]	5.67 × 10^{-3} (0.9 %)	2.92 × 10^{-3} (1.3 %)	9.02 × 10^{-3} (1.8 %)
k [s]	0.36 (10.2 %)	0.32 (18.9 %)	7.40 (6.2 %)
R_W [Ω cm²]	530 (3.5 %)	872 (4.0 %)	394 (2.1 %)
τ_D [s]	0.36 (35.3 %)	26.38 (29.9 %)	44.19 (9.5 %)
ϕ	0.45 (3.9 %)	0.36 (3.2 %)	0.28 (1.0 %)
R [Ω cm²]	10.42 (3.7 %)	12.88 (5.2 %)	24.56 (2.4 %)
C [F cm^{-2}]	1.20 × 10^{-2} (5.6 %)	2.83 × 10^{-3} (7.6 %)	4.69 × 10^{-3} (3.8% %)
χ^2	3.3 × 10^{-4}	5.0 × 10^{-4}	4.2 × 10^{-4}

The compaction of Y-112 during oxidation imposes a partial irreversible character of this process, and as a consequence the oxidation leads to disappearance of the oxidation plateau and also to the attenuation of the reduction peak.

Impedance measurements during $YBaCo_2O_5$ oxidation indicate the presence of a chemical step tentatively assigned to the formation of O^{2-} ions from the reaction between two hydroxyl groups and a diffusion process of oxygen ions from the surface to the bulk of the mixed conductor.

References

Aurelio G., Curiale, J., Sanchez, R. D., Cuello, G. J., (2007), Effects on the physical properties of cation substitution in the layered cobaltites, *Physica B: Condensed Matter*, **398**, 223-228.

Bebelis S., Kotsionopoulos, N., Mai, A., Tietz, F., (2007), Electrochemical characterization of perovskite-based SOFC cathodes, *Journal of Applied Electrochemistry*, **37**, 15-20.

Bobrovskii V., Kazantsev, V., Mirmelstein, A., Mushnikov, N., Proskurnina, N., Voronin, V., Pomjakushina, E., Conder, K., Podlesnyak, A., (2009), Spontaneous and field-induced magnetic transitions in $YBaCo_2O_{5.5}$, *Journal of Magnetism and Magnetic Materials*, **321**, 429-437.

Dan M., Pralong V., Vaszilcsin N., Kellenberger A., Duteanu N., (2011), Electrochemical behaviour of $YBaCo_4O_7$ in alkaline aqueous solution, *Journal of Solid State Electrochemistry*, **15**, 1227-1233.

Doubova L., Barison S., Boldrini S., Fabrizio M., MortalĂ C., Pagura C., (2009), Conductivity studies of sol-gel prepared $BaCe_{0.85-x}Zr_xY_{0.15}O_{3-\delta}$ solid electrolytes using impedance spectroscopy, *Journal of Applied Electrochemistry*, **39,** 2129-2141.

González-Cuenca M., Zipprich W., Boukamp B. A., Pudmich G., Tietz F., (2001), Impedance Studies on Chromite-Titanate Porous Electrodes under Reducing Conditions, *Fuel Cells*, **1,** 256-264.

Green R.D., Liu C.-C., Adler S.B., (2008), Carbon dioxide reduction on gadolinia-doped ceria cathodes, *Solid State Ionics*, **179,** 647-660.

Grenier J.C., Bassat J.M., Doumerc J.P., Etourneau J., Fang Z., Fournes L., Petit S., Pouchard M., Wattiaux A., (1999), Relevant examples of intercalation-deintercalation processes in solid state chemistry: application to oxides, *Journal of Materials Chemistry*, **9**, 25-33.

Grenier J.C., Wattiaux A., Doumerc J.P., Dordor P., Fournes L., Chaminade J.P., Pouchard M., (1992), Electrochemical oxygen intercalation into oxide networks, *Journal of Solid State Chemistry*, **96**, 20-30.

Haoshan H., Lu Z., Yingfang W., Shijiang L., Xing H., (2007), Thermogravimetric Study on Oxygen Adsorption/Desorption Properties of Double Perovskite Structure Oxides $REBaCo_2O_{5+\delta}$ (RE = Pr, Gd, Y), *Journal of Rare Earths*, **25**, 275-281.

Kim J.-H., Manthiram, A., (2008), $LnBaCo_2O_{5+\delta}$ Oxides as Cathodes for Intermediate-Temperature Solid Oxide Fuel Cells, *Journal of The Electrochemical Society*, **155**, B385-B390.

Kim J.-S., Pyun S.-I., Lee J.-W., Song R.-H., (2007), Kinetics of oxygen reduction on porous mixed conducting $(La_{0.85}Sr_{0.15})_{0.9}MnO_3$ electrode by ac-impedance analysis, *Journal of Solid State Electrochemistry*, **11**, 117-125.

Levi M. D., Gizbar H., Lancry E., Gofer Y., Levi E., Aurbach D., (2004), A comparative study of Mg^{2+} and Li^+ ion insertions into the Mo_6S_8 Chevrel phase using electrochemical impedance spectroscopy, *Journal of Electroanalytical Chemistry*, **569**, 211-223.

Liu Y., (2009), $YBaCo_2O_{5+\delta}$ as a new cathode material for zirconia-based solid oxide fuel cells, *Journal of Alloys and Compounds*, **477**, 860-862.

Lv H., Zhao B.-Y., Wu Y.-J., Sun G., Chen G., Hu, K.-A., (2007), Effect of B-site doping on $Sm_{0.5}Sr_{0.5}M_xCo_{1-x}O_{3-\delta}$ properties for IT-SOFC cathode material (M = Fe, Mn), *Materials Research Bulletin*, **42**, 1999-2012.

Nielsen J., Jacobsen T., Wandel M., (2011), Impedance of porous IT-SOFC LSCF:CGO composite cathodes, *Electrochimica Acta*, **56**, 7963-7974.

Pelosato R., Donazzi A., Dotelli G., Cristiani C., Natali Sora I., Mariani M., Electrical characterization of co-precipitated $LaBaCo_2O_{5+\delta}$ and $YBaCo_2O_{5+\delta}$ oxides, *Journal of European Ceramic Society*, **34**, 4257-4272.

Sajana T.K., Ghangrekar M.M., Mitra A., (2017), Influence of electrode material on performance of sediment microbial fuel cell remediating aquaculture water, *Environmental Engineering and Management Journal*, **16**, 421-429.

Tarancon A., Burriel M., Santiso J., Skinner S. J., Kilner J. A., (2010), Advances in layered oxide cathodes for intermediate temperature solid oxide fuel cells, *Journal of Materials Chemistry*, **20**, 3799-3813.

Therese G. H. A., Dinamani M., Vishnu Kamath P., (2005), Electrochemical synthesis of perovskite oxides, *Journal of Applied Electrochemistry*, **35**, 459-465.

Wackerl J., Koppitz T., Peck D.-H., Woo S.-K., Markus T., (2009), Correlation of thermal properties and electrical conductivity of La0.7Sr0.3Cu0.2Fe0.8O3âˆ’Î´ material for solid oxide fuel cells, *Journal of Applied Electrochemistry*, **39**, 1243-1249.

Zhang K., Ge L., Ran R., Shao Z., Liu S., (2008), Synthesis, characterization and evaluation of cation-ordered $LnBaCo_2O_{5+\delta}$ as materials of oxygen permeation membranes and cathodes of SOFCs, *Acta Materialia*, **56**, 4876-4889.

Zhang X., Hao H., He Q., Hu X., (2007), High-temperature electronic transport properties of Fe-doped $YBaCo_2O_{5+\delta}$, *Physica B: Condensed Matter*, **394**, 118-121.